

One- and Two-Metal Ion Catalysis of the Hydrolysis of Adenosine 3'-Alkyl Phosphate Esters. Models for One- and Two-Metal Ion Catalysis of RNA Hydrolysis

Thomas C. Bruice,* Akira Tsubouchi, Robert O. Dempcy, and Leif P. Olson

Contribution from the Department of Chemistry, University of California at Santa Barbara, Santa Barbara, California 93106

Received March 6, 1996[⊗]

Abstract: Adenosine 3'-O(PO₂⁻)OCH₂R phosphate esters have been synthesized with R = 8-hydroxyquinol-2-yl (**1a**) and 8-(hydroxyquinolyl)-2-methylene (**1b**). The adenosine 3'-O(PO₂⁻)OCH₂R structure has the essential features of an RNA dinucleotide. Equilibrium binding studies with metal ions Mg²⁺, Zn²⁺, Cu²⁺, and La³⁺ have been carried out with **1a**, **1b**, HOCH₂R (**7a** and **7b**), and 8-hydroxyquinoline (**8**), and equilibrium constants (*K*_{as}) have been determined for the formation of 1:1 (L)Mⁿ⁺ complexes. The hydrolysis of **1a** and **1b** as well as (1a)Mⁿ⁺ and (1b)Mⁿ⁺ species are first order in HO⁻. The rate enhancement for hydrolysis of **1a** by complexation with metal ions is as follows: ~10⁵ with Zn²⁺, ~10³ with Mg²⁺, ~10⁵ with Cu²⁺, and ~10⁹ with La³⁺. Molecular modeling indicates that metal ions ligated to the 8-hydroxyquinoline moiety in the complexes (1a)Mⁿ⁺ and (1b)Mⁿ⁺ catalyze **1a** and **1b** hydrolysis by interacting as Lewis acid catalysts with the negatively charged oxygen atom of the phosphate group. In the instance of La³⁺ complexes, the ligated metal ion is within an interactive distance with both the negative phosphate oxygen and the leaving oxygen. This bimodal assistance by La³⁺ to the displacement reaction at phosphorus by the 2'-hydroxyl anion results in remarkable rate accelerations for the hydrolysis of (1a)La³⁺ and (1b)La³⁺ complexes. The complexes (1a)Mⁿ⁺ and (1b)Mⁿ⁺ are themselves hydrolyzed by metal ion catalysis in a reaction that is first order in HO⁻, an observation consistent with a transition state composition of [(1a,b)Mⁿ⁺][Mⁿ⁺][HO⁻]. We assume the kinetic equivalent [(1a,b)Mⁿ⁺][Mⁿ⁺OH] to represent the reacting species. In this catalysis the Mⁿ⁺OH is proposed to play the role of general base to deprotonate the 2'-OH while the metal in the complexes (1a,b)Mⁿ⁺ is coordinated to a negative oxygen of the -(PO₂⁻)- moiety. This double metal ion catalysis mimics a mechanism proposed for the ribozyme self-cleavage of RNA.

Introduction

The half-life for the hydrolysis of dialkyl phosphate esters at neutrality exceeds the normal lifespan of a human.¹ The mere existence of enzymes capable of rapidly hydrolyzing DNA establishes the existence of chemical mechanisms for facile phosphodiester bond hydrolysis. Hydrolysis of RNA is much more rapid in both chemical and enzymatic processes due to anchimeric assistance of the ribose 2'-hydroxyl group. There has been intensive interest in mechanisms of hydrolysis of phosphodiester esters owing to implications in enzyme hydrolysis of DNA and RNA. A number of phosphoesterases and ribozymes have been shown to require two or more metal ions for their catalytic activity. Two metal ions have been shown to be required for activity by the 3',5'-exonuclease from the Klenow fragment of *Escherichia coli* DNA polymerase I,² *E. coli* alkaline phosphatase,³ phospholipase C from *Bacillus cereus*,⁴ RNase H from HIV reverse transcriptase,⁵ and hammerhead ribozyme.⁶ Metal ions have been proposed to play three essential roles in the catalytic processes: (i) due to the decrease

in the p*K*_a of H₂O upon binding to metal ions, metal bound hydroxide ion is generated and acts as the nucleophile, or in the case of RNA hydrolysis, acts as a base to generate 2'-O⁻, which acts as the nucleophile; (ii) ligation of the metal ion at a negative oxygen of the -(PO₂⁻)- linker to increase the latter's electrophilic susceptibility to nucleophilic attack; and (iii) assistance of departure by interaction of metal ion in the transition state with the partial negative charge on leaving oxygen.

It is appreciated that many metal ions promote the transesterification of RNA, for example, Zn²⁺,⁷ Ni²⁺,^{7c} Co²⁺,^{7f,g} Cu²⁺,^{7f,g,8} Mg²⁺,⁹ Mn²⁺,^{7f,g,10} Pb²⁺,¹¹ Al³⁺,^{7b} La³⁺.¹² There is still a great deal to know about these reactions. Kinetic studies directed at the determination of the mechanism of metal ion

[⊗] Abstract published in *Advance ACS Abstracts*, October 1, 1996.

(1) Westheimer, F. H. In *Phosphorus Chemistry, Development in American Science*; Walsh, E. N., Griffith, E. J., Parry, R. W., Quin, L. D., Eds.; ACS Symposium Series; American Chemical Society: New York, 1992.

(2) Beese, L. S.; Steitz, T. A. *EMBO J.* **1991**, *10*, 25.

(3) Kim, E. E.; Wyckoff, H. W. *J. Mol. Biol.* **1991**, *218*, 449.

(4) Hough, E.; Hansen, L. K.; Briknes, B.; Jynge, K.; Hansen, S.; Hordrik, A.; Little, C.; Dodson, E.; Derewenda, Z. *Nature* **1989**, *338*, 357.

(5) Davies, J. F.; Hostomska, Z.; Jordan, S. R.; Matthews, D. A. *Science* **1991**, *252*, 88.

(6) (a) Steitz, T. A.; Steitz, J. A. *Proc. Natl. Acad. Sci. U.S.A.* **1993**, *90*, 6498. (b) Piccirilli, J. A.; Vyle, J. S.; Caruthers, M. H.; Cech, T. R. *Nature (London)*, **1993**, *361*, 85.

(7) (a) Rorodorf, B. F.; Kearns, D. R.; *Biopolymers* **1976**, 1491. (b) Dimroth, K.; Witzel, H.; Hulsen, W.; Mirbach, H. *Justus Liebig's Ann. Chem.* **1959**, 620, 94. (c) Stern, M. K.; Bashkin, J. K.; Sall, E. D. *J. Am. Chem. Soc.* **1990**, *112*, 5357. (d) Eichhorn, G. L.; Butzow, J. J. *Biochemistry* **1971**, *10*, 2014. (e) Butzow, J. J.; Eichhorn, G. L. *Biochemistry* **1971**, *10*, 2019. (f) Butzow, J. J.; Eichhorn, G. L. *Biopolymers* **1965**, *3*, 95. (g) Ikenaga, H.; Inoue, Y. *Biochemistry* **1975**, *13*, 577.

(8) Modak, A. S.; Gard, J. K.; Merriman, M. C.; Winkler, K. A.; Bashkin, J. K.; Stern, M. K. *J. Am. Chem. Soc.* **1991**, *113*, 283.

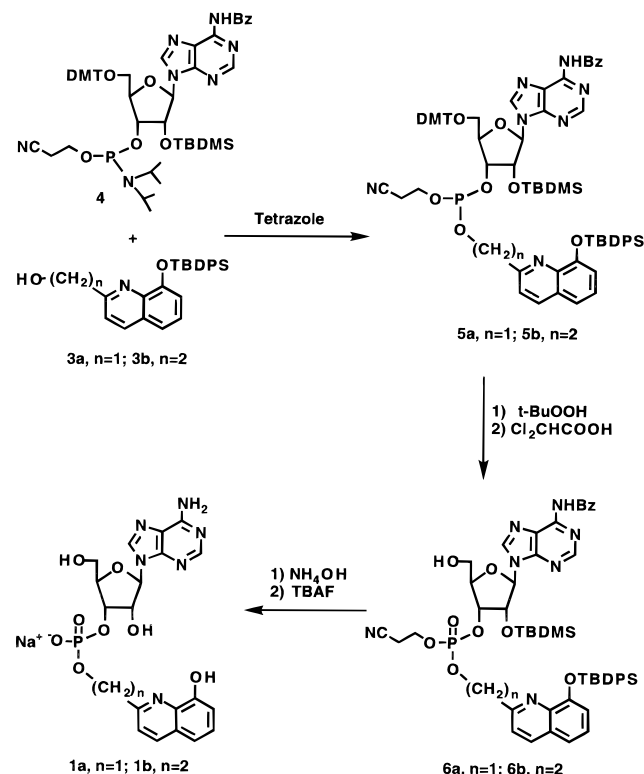
(9) Wintermeyer, W.; Zachau, H. G. *Biochim. Biophys. Acta* **1973**, *299*, 82.

(10) Dange, V.; Van Atta, R. B.; Hecht, S. M. *Science* **1990**, *248*, 585.

(11) (a) Werner, C.; Krebs, B.; Keith, G.; Dieheimer, G. *Biochim. Biophys. Acta* **1976**, *432*, 161. (b) Brown, R. S.; Hingerty, B. E.; Dewan, J. C. *Nature* **1983**, *303*, 543. (c) Brown, R. S.; Dewan, J. C.; Klug, A. *Biochemistry* **1985**, *24*, 4785. (d) Behlen, L. S.; Sampson, J. R.; Drenzo, A. B.; Uhlenbeck, O. C. *Biochemistry* **1990**, *29*, 2515. (e) Farkas, W. R. *Biochim. Biophys. Acta* **1967**, *155*, 401. (f) Morrow, J. R.; Buttrey, L. A.; Shelton, V. M.; Berback, K. A. *J. Am. Chem. Soc.* **1992**, *114*, 1903.

(12) (a) Eichhorn, G. L.; Butzow, J. J. *Biopolymers* **1965**, *3*, 79. (b) Baumann, E.; Trapman, H.; Fischler, F. *Biochem. Z.* **1954**, 328.

Scheme 1



catalysis are often compromised by the formation of insoluble nucleotide metal ion complexes, the precipitation of metal hydroxides, formation of metal hydroxide gels, and the complexity of the reaction system. Substrates that have been employed as RNA models to test the catalytic activities of various metal ions¹³ include dinucleotides such as UpU and ApA. Recently, several designed ligands capable of complexing two metals have been reported to catalyze the transesterification of dinucleotides by cooperation of both metal ions.¹⁴ Lanthanum ion and its complexes have attracted attention as catalysts for phosphate ester hydrolysis in this¹⁵ and many other laboratories¹⁶ because of the high efficiency of La³⁺ catalysis.

We have now synthesized phosphate diesters **1a** and **1b** (Scheme 1) and studied the influence of Cu²⁺, Zn²⁺, Mg²⁺, and La³⁺ on the rates of their hydrolyses. Phosphate esters **1a** and **1b** were designed to allow modeling of the influence of metal ions on RNA hydrolysis. The 8-hydroxyquinoline moieties of **1a** and **1b** serve to place a metal ion at variable distance to the $-(\text{PO}_2^-)-$ function, the leaving oxygen, and nucleophilic 2'-hydroxyl group.

A part of this work has been reported in our preliminary paper.¹⁷

(13) (a) Linkletter, B.; Chin, J. *Angew. Chem., Int. Ed. Engl.* **1995**, *34*, 472. (b) Breslow, R.; Huang, D.-L.; Anslyn, E. *Proc. Natl. Acad. Sci. U.S.A.* **1989**, *86*, 1746. (c) Breslow, R.; Huang, D.-L. *Proc. Natl. Acad. Sci. U.S.A.* **1991**, *88*, 4080. (d) Shelton, V. M.; Morrow, J. R. *Inorg. Chem.* **1991**, *30*, 4295. (e) Irisawa, M.; Takeda, N.; Komiyama, M. *J. Chem. Soc., Chem. Commun.* **1995**, 1221. (f) Kuusela, S.; Rantanen, M.; Lönnberg, H. *J. Chem. Soc., Perkin Trans. 2* **1995**, 2269.

(14) (a) Yashiro, M.; Ishikubo, A.; Komiyama, M. *J. Chem. Soc., Chem. Commun.* **1995**, 1793. (b) Young, M. J.; Chin, J. *J. Am. Chem. Soc.* **1995**, *117*, 10577. (c) Chapman, W. H., Jr.; Breslow, R. *J. Am. Chem. Soc.* **1995**, *117*, 5462.

(15) (a) Tsubouchi, A.; Bruce, T. C. *J. Am. Chem. Soc.* **1994**, *116*, 11614. (b) Tsubouchi, A.; Bruce, T. C. *J. Am. Chem. Soc.* **1995**, *117*, 7399.

(16) (a) Komiyama, M.; Matsumura, K.; Matsumoto, Y. *J. Chem. Soc., Chem. Commun.* **1992**, 640. (b) Takasaki, B. K.; Chin, J. *J. Am. Chem. Soc.* **1993**, *115*, 9337. (c) Morrow, J. R.; Buttrey, L. A.; Berback, K. A. *Inorg. Chem.* **1992**, *31*, 16. (d) Breslow, R.; Zhang, B. *J. Am. Chem. Soc.* **1994**, *116*, 7894.

Experimental Section

Materials. 8-[(*tert*-Butyldiphenylsilyloxy)-2-methylquinoline (**2**) and [8-[(*tert*-butyldiphenylsilyloxy)quinolyl]methanol (**3a**) were prepared according to the method previously reported.^{15b} All reagents for syntheses were purchased from commercial vendors and used without further purification. All solvents were dried over proper drying agents and distilled before use. Buffers and metal chlorides were of highest purity available and used as received from the suppliers. Solutions of KCl, used to maintain constant ionic strength, were demetalated by filtration through a Chelex 100 resin (Bio-Rad) column. Glass-distilled deionized water was used for all kinetic and equilibrium studies. ¹H NMR spectra were recorded on a Varian Gemini-200 or a General Electric GN-500 spectrometer with tetramethylsilane as an internal standard. When deuterium oxide (D₂O) or deuterated dimethyl sulfoxide (DMSO-*d*₆) was used as a solvent, the chemical shifts were reported relative to the signal of the solvent (D₂O, 4.63 ppm; DMSO-*d*₆, 2.50 ppm). IR spectra were obtained on a Perkin-Elmer 1330 spectrophotometer. High-resolution mass spectrometry was performed at the University of California, Los Angeles, Mass Facility.

Preparation of Phosphodiesters. Adenosine 3'-[(8-Hydroxyquinolyl)methyl phosphate] (1a**).** Tetrazole (125 mg, 1.78 mmol) was added to a solution of *N*⁶-benzoyl-5'-(4, 4'-dimethoxytrityl)-2'-(*tert*-butyldimethylsilyl)adenosine-3'-[β-(cyanoethyl)-*N,N*-diisopropylphosphoramidite] (**4**) (500 mg, 0.508 mmol) in dry acetonitrile (5 mL) under argon, and the solution was stirred at room temperature for 20 min. To this solution was added a solution of the alcohol **3a** (214 mg, 0.518 mmol) in dry acetonitrile (5 mL). The resulting solution was stirred for 90 min at 25 °C and then evaporated. The residue, containing the coupling product, was dissolved in methylene chloride (4 mL) and cooled to 0 °C. A solution of 3 M *tert*-butyl hydroperoxide in 2,4,4-trimethylpentane (0.65 mL, 1.95 mmol) was added, and the resulting solution was stirred for 30 min at 0 °C. To this solution was added 50 mL of 2% dichloroacetic acid in methylene chloride. The solution was stirred for 2 min at room temperature and then poured into 50 mL of 5% sodium bicarbonate solution. The organic layer was separated, and the aqueous layer was extracted with methylene chloride (2 × 50 mL). The organic extracts were combined, dried over sodium sulfate, and concentrated. The residue was chromatographed through a silica gel column eluting with 5% methanol in ethyl acetate to afford the diastereomers of **6a**. To a solution of the crude product in ethanol (4 mL) was added 40 mL of ammonium hydroxide, and the mixture was heated at 60 °C for 1 h. After the mixture was cooled to room temperature, the reaction solution was evaporated by codistillation with absolute ethanol. Addition of ethyl acetate to the residue afforded the 2'-(*tert*-butyldimethylsilyl)-protected nucleotide as a white solid (188 mg, 54% for the four step process): mp > 120 °C (slow dec); IR (KBr) 3162, 1687, 1649, 1604, 1475, 1432, 1214, 1076, 838 cm⁻¹; ¹H NMR (DMSO-*d*₆) δ 9.10 (s, 1H, phenol), 8.37 and 8.13 (2 × s, 2H, purine ArH), 8.22 (d, *J* = 8.5 Hz, 1H, quinoline ArH), 7.65 (d, *J* = 8.5 Hz, 1H, quinoline ArH), 7.42 (br s, 2H, -NH₂), 7.38 (m, 2H, quinoline ArH), 7.07 (dd, *J* = 2.4, 6.7 Hz, 1H, quinoline ArH), 5.91 (d, *J* = 5.2 Hz, 1H, 1'-H), 5.06 (d, *J*_{PH} = 7.6 Hz, 2H, -POCH₂-), 4.69 (m, 1H, 2'-H), 4.64 (m, 1H, 3'-H), 4.30 (m, 1H, 4'-H), 3.7–3.56 (m, 2H, 5'-H), 3.11 and 2.86 (2 × t, 4H, *J* = 6.7 Hz, NCC₂H₂NH₃⁺), 0.68 (s, 9H, -SiC(CH₃)₃), -0.12 and -0.20 (2 × s, 6H, -SiCH₃); HRMS (FAB) *m/z* 619.2102 (calcd for C₂₆H₃₆N₆O₈PSi (M + H)⁺ 619.2104).

To a solution of the above nucleotide (188 mg, 0.273 mmol) in THF (6 mL) was added 2.7 mL of 1 M tetrabutylammonium fluoride in THF. After the solution was stirred for 1 h at room temperature, the solvent was evaporated. The residue was dissolved in a minimum amount of water and filtered through a column of Bio-Rex 70 cation exchange resin (sodium form) eluting with water. The fraction containing the nucleotide was concentrated, and the residue was chromatographed through a column of Bakerbond phenyl reversed-phase gel eluting with 50% methanol in water. Nucleotide **1a** was isolated and precipitated from ethanol-hexane (108 mg, 75%): mp > 165 °C (slow dec); IR (KBr) 3390, 3218, 1649, 1604, 1238, 1081 cm⁻¹; ¹H NMR (DMSO-*d*₆) δ 9.64 (br s, 1H, phenol), 8.36 and 8.11 (2 × s, 2H, purine ArH), 8.30 (d, *J* = 8.6 Hz, 1H, quinoline ArH), 7.70 (d, *J* = 8.6 Hz, 1H, quinoline ArH), 7.41 (m, 2H, quinoline ArH),

(17) Dempcy, R. O.; Bruce, T. C. *J. Am. Chem. Soc.* **1994**, *116*, 4511.

7.07 (dd, $J = 2.8, 6.0$ Hz, 1H, quinoline ArH), 5.88 (d, $J = 6.4$ Hz, 1H, 1'-H), 5.59 (br s, 1H, 2'-hydroxyl), 5.05 (d, $J_{\text{PH}} = 7.7$ Hz, 2H, $-\text{POCH}_2-$), 4.64 (m, 2H, 2'- and 3'-H), 4.04 (m, 1H, 4'-H), 3.48 (m, 2H, 5'-H); HRMS (FAB) m/z 505.1237 (calcd for $\text{C}_{20}\text{H}_{22}\text{N}_6\text{O}_8\text{P}$ ($\text{M} + \text{H}$)⁺ 505.1239).

Adenosine 3'-[2-(8-Hydroxyquinolyl)ethyl phosphate] (1b). To a solution of 8-[(*tert*-butyldiphenylsilyloxy)-2-methylquinoline (**2**) (3.0 g, 7.5 mmol) in dry THF (30 mL) was slowly added *n*-butyllithium (10 mmol, 1.6 M in hexane) at -20 °C. After being stirred for 1 min, the reaction mixture was warmed quickly to 0 °C, and gaseous formaldehyde (generated by thermal cracking of paraformaldehyde at ~ 200 °C and entrained in a flow of nitrogen) was bubbled rapidly into the solution until the red color of the carbanion was discharged, ca. 5 min. The mixture was then poured into 100 mL of 5% aqueous NaHCO_3 , and the product was extracted with ether. The separated organic phase was dried over Na_2SO_4 and the solvent removed by rotary evaporation. The crude product was purified by column chromatography on silica gel (75:25 hexane/ethyl acetate) to give 2-[8-[(*tert*-butyldiphenylsilyloxy)quinolyl]ethanol (**3b**) as a viscous yellow oil: ^1H NMR (CDCl_3) δ 8.08 (d, $J = 8.5$ Hz, 1H, quinoline ArH), 7.79 (d, $J = 7.8$ Hz, 4H, phenyl), 7.42–7.27 (m, 8H, phenyl and quinoline ArH), 7.90 (t, $J = 7.9$ Hz, 1H, quinoline ArH), 6.75 (d, $J = 8.5$ Hz, 1H, quinoline ArH), 5.10 (br s, 1H, OH), 4.12 (t, $J = 5.3$ Hz, 2H, $\text{CH}_2\text{CH}_2\text{OH}$), 3.16 (t, $J = 5.3$ Hz, 2H, $\text{CH}_2\text{CH}_2\text{OH}$), 1.18 (s, 9H, $-\text{SiC}(\text{CH}_3)_3$); ^{13}C NMR (CDCl_3) δ 160.12, 151.05, 140.30, 136.40, 135.36, 132.70, 129.75, 128.15, 127.68, 125.80, 121.97, 119.84, 117.22, 61.03, 60.33, 38.80, 26.30, 20.98, 19.56, 14.12, 0.97; IR (KBr) 3350 (OH), 3100, 3035, 3025, 2985, 2960, 2845, 1820, 1785, 1750, 1675, 1670, 1590, 1510, 1480, 1450, 1370, 1310, 1265, 1200, 1105, 945 cm^{-1} ; HRMS (CI; NH_3) m/z 428.2046 (calcd for $\text{C}_{27}\text{H}_{30}\text{NO}_2\text{Si}$ ($\text{M} + \text{H}^+$) 428.2048). The desired nucleotide **1b** was prepared from the alcohol **3b** (225 mg, 0.53 mol) as described for **1a**. The pure nucleotide **1b** (110 mg, 38% based on **3b** for the whole process) was obtained as a white solid: dec >140 °C; IR (KBr) 3363, 3210, 1649, 1602, 1243, 1087 cm^{-1} ; ^1H NMR δ 8.36 and 8.13 ($2 \times$ s, 1H, purine ArH), 8.13 (d, $J = 8.4$ Hz, 1H, quinoline ArH), 7.38 (t, $J = 7.4$ Hz, 1H, quinoline ArH), 7.38 (br s, 2H, NH_2), 7.30 (d, $J = 7.9$ Hz, 1H, quinoline ArH), 7.15 (d, $J = 8.0$ Hz, 1H, quinoline ArH), 6.91 (d, $J = 7.3$ Hz, 1H, quinoline ArH), 5.86 (d, $J = 6.9$ Hz, 1H, 1'-H), 4.60 (m, 2H, 2'- and 3'-H), 4.25 (m, 2H, POCH_2CH_2), 4.03 (m, 1H, 4'-H), 3.56 (m, 2H, 5'-H), 3.21 (t, $J = 6.0$ Hz, 2H, POCH_2CH_2); LRMS (FAB) m/z 518.3 (calcd for $\text{C}_{21}\text{H}_{23}\text{N}_6\text{O}_8\text{P}$ ($\text{M} + \text{H}^+$) 518.4).

Kinetic Measurements. The ionic strength of the reaction solutions was maintained at 1.0 with KCl. Buffers (0.1 M) were used within 1 pH unit of their pK_a values to maintain constant pH; the buffers employed were MES (2-(*N*-morpholino)ethanesulfonic acid), HEPES (*N*-(2-hydroxyethyl)piperazine-*N'*-3-propanesulfonic acid), CHES ((2-cyclohexylamino)ethanesulfonic acid), CAPS (3-(cyclohexylamino)-1-propanesulfonic acid), phosphate, with pH adjusted by addition of KOH. EDTA (10 mM) was incorporated into buffer solutions for nonmetal ion-assisted reactions to sequester trace metal ion impurities. The pH values of the buffer solutions were measured with a Radiometer Model 26 pH meter and a combination glass electrode.

The hydrolysis of **1a** and **1b** in the presence and absence of metal ions, except for hydrolysis promoted by La^{3+} , was followed by HPLC. A Perkin-Elmer series 100 pump module equipped with an Alltima C18 analytical column (Alltech) was used, and chromatograms were recorded on a Hewlett-Packard HP 3392A integrator connected to a Hewlett-Packard HP 1050 variable-wavelength detector set at 260 nm. Kinetic runs were initiated by adding 5–10 μL of the nucleotide stock solution into 1.5 mL of the buffer solution thermally equilibrated at 30 °C to give the final concentration of 10 μM in **1a,b**. Aliquots of the reaction solutions were periodically injected (50 μL) on the HPLC column. The samples were eluted with 20% acetonitrile for **1a** and 15% acetonitrile for **1b** in 50 mM potassium phosphate buffer (pH 3.4) at a flow rate of 1.0 mL/min. Disappearance of the nucleotides **1a,b** was monitored. The reactions followed pseudo-first-order kinetics for at least 4 half-lives. The pseudo-first-order rate constants (k_{obsd}) were evaluated by fitting the first-order-rate law (eq 1) to the plots of

$$A = A_0 e^{-k_{\text{obsd}} t} \quad (1)$$

the integrated area (A_t) of the nucleotide peak vs time (t) where A_0 is the integrated peak area at $t = 0$.

The rates of the hydrolysis of **1a** in the presence of La^{3+} were measured by the stopped-flow method using an OLIS RMS-1000 rapid-scanning stopped-flow system thermostated at 30 °C. One driving syringe contained LaCl_3 in buffer solution (0.1 M), and the other driving syringe contained the substrate (20 μM) in the same buffer solution (0.1 M). Ionic strength was held constant at 1.0 with KCl. The reactions were followed by monitoring the change of the absorbance at 260 nm. The collected data points were fit to theoretical curves by software written for OLIS RSM (rapid-scanning monochromator) to give the pseudo-first-order rate constants.

For the hydrolysis of **1b** in the presence of La^{3+} , the reactions were performed in quartz cuvettes (1 cm path length), thermostated at 30 °C, containing solutions (3 mL) of buffer and LaCl_3 . The reactions were initiated by adding the stock solution of **1b** to the buffer solution to give the final concentration of 10 μM in **1b**. The change of the absorbance (A) at 260 nm was followed by a Perkin-Elmer 553 spectrophotometer. The pseudo-first-order rate constants were obtained by fitting the theoretical equation for a first-order process to the data points of plots of A vs time.

Metal Binding Equilibria. The equilibrium constants for binding of the nucleotides **1a** and **1b**, corresponding leaving alcohols **7a** and **7b**, and 8-hydroxy-2-methylquinoline (**8**) with metal ions were spectrophotometrically determined at 30 °C ($\mu = 1.0$ with KCl). Buffer solutions (3 mL, 0.1 M) of substrates (10 μM) in thermostated cuvettes were titrated with metal chloride solutions of known concentration and the absorbances (A) at 260 and 243 nm were recorded on a Perkin-Elmer 553 spectrophotometer. The volume of titrant added was 50 μL , less than 2% of that of the buffered solutions of **1a**, **1b**, **7a**, **7b**, and **8**.

Spectrophotometric pH Titration. The pK_a (phenolic proton ionization) of the nucleotides **1a** and **1b** and corresponding leaving alcohols **7a** and **7b** and phenol **8** were determined spectrophotometrically at 30 °C ($\mu = 1.0$ with KCl). The absorbances of the solutions of substrates (20 μM) were recorded at 234 and 260 nm with the pH varied from 8.3 to 11.3 and also at pH 7 and 12. All solutions were buffered with CAPS (0.05 M) except for those with pH 7 (HEPES) and pH 12 (KOH). In order to determine pK_a values, plots of the absorbances at two wavelengths were fit by the theoretical equation for the dissociation of a monoprotic acid. The values obtained at 234 and 260 nm were averaged.

Results

The preparation of adenosine (8-hydroxyquinolyl)methyl phosphate (**1a**) and adenosine 2-(8-hydroxyquinolyl)ethyl phosphate (**1b**) is illustrated in Scheme 1. Coupling of the alcohols **3a,b** with *N*⁶-benzoyl-5'-(4, 4'-dimethoxytrityl)-2'-(*tert*-butyldimethylsilyl)adenosine 3'-(β -cyanoethyl *N,N*-diisopropylphosphoramidite) (**4**) in the presence of triazole afforded the intermediates **5a,b**. Oxidation of **5a,b** with *tert*-butyl hydroperoxide followed by removal of the 5'-dimethoxytrityl protecting group with 2% dichloroacetic acid in methylene chloride yielded the diastereomers of **6a,b**. These diastereomers were converted into the tetrabutylammonium salts of target nucleotides **1a** and **1b** by cleavage of the cyanoethyl, the *N*⁶-benzoyl, and the *tert*-butyldiphenylsilyl groups with ammonium hydroxide, followed by deprotection of the 2'-*tert*-butyldimethylsilyl group with tetrabutylammonium fluoride (TBAF). The sodium salts of **1a** and **1b** were obtained by cation-exchange chromatography.

Metal Binding Studies. Association constants for the metal ion complexes of **1a** and **1b**, in addition to their corresponding leaving alcohols **7a** and **7b**, with Zn^{2+} , Mg^{2+} , Cu^{2+} , and La^{3+} were determined at constant pH by spectrophotometric titration (30 °C; $\mu = 1.0$ with KCl). As a control, complexation of 8-hydroxy-2-methylquinoline (**8**) was also examined. Typical

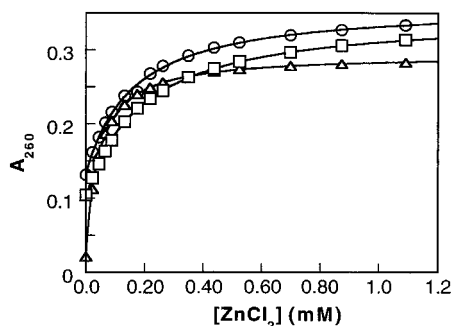
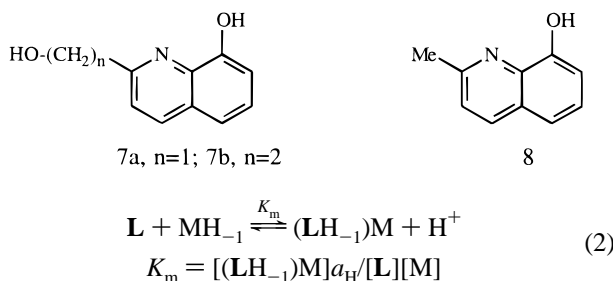


Figure 1. Plots of absorbance of **1a** (□), **7a** (△), and **8** (○) at 260 nm vs $[\text{Zn}^{2+}]$ at 30 °C ($\mu = 1.0$) and pH 6.17. The solid lines best fit to the data points were generated by use of eq 3.

plots of A_{260} vs metal ion concentration are provided in Figure 1 for titration of **1a**, **7a**, and **8** with ZnCl_2 at pH 6.17. Apparent association constants (K_m), defined in eq 2, were obtained from



$\text{L} = \mathbf{1a}, \mathbf{1b}, \mathbf{7a}, \mathbf{7b},$ or **8**, $\text{M} = \text{Zn}^{2+}, \text{Mg}^{2+}, \text{Cu}^{2+},$ or La^{3+}

the nonlinear least-squares fit of A_{260} vs $[\text{M}^{n+}]$ by use of eq 3. In eq 3, A_0 and A_1 refer to the absorbances of the solution at $[\text{M}^{n+}] = 0$ and at saturation upon complexation, respectively, $[\text{M}^{n+}]$ the concentration of unbound metal ion, and a_{H} proton activity. Equation 3 was derived by combination of eq 2 and mass balance in terms of the ligands.

$$A = \frac{(A_0 a_{\text{H}} + A_1 K_m [\text{M}^{n+}])}{(a_{\text{H}} + K_m [\text{M}^{n+}])} \quad (3)$$

In the curve fitting, $[\text{M}^{n+}]$ can be replaced by the total concentration of metal ion ($[\text{M}^{n+}]_{\text{T}}$) due to $[\text{M}^{n+}]_{\text{T}} \gg [\text{L}]$. The lines in Figure 1 are the best fits of A_{260} vs $[\text{ZnCl}_2]$ using eq 3. The values of K_m providing the best fit were converted into those of K_{as} by dividing by the acid dissociation constants K_{a} (Table 1) of the phenolic proton of the **1a**, **7a**, and **8** ligands (eq 4).

$$K_{\text{as}} = K_m / K_{\text{a}} = \frac{[(\text{LH}_{-1})\text{M}]}{[\text{LH}_{-1}][\text{M}]} \quad (4)$$

The values of $\log K_{\text{as}}$ for other metal ions were calculated in the same manner used for Zn^{2+} complexes (plots of A_{260} vs $[\text{M}]$ are not shown). The K_{as} values calculated from the plots of A_{260} vs $[\text{M}]$ were consistent with those evaluated from the plots of the absorbance at another wavelength (243 nm). The values of $\log K_{\text{as}}$ in Table 1 are the average of numbers determined at two wavelengths. Due to the rapid hydrolysis of **1a** and **1b** in the presence of La^{3+} , the thermodynamic values of the association constants for formation of La^{3+} complexes could not be determined.

Because the K_m values for the copper complexes are so large, they could not be determined *via* our spectrophotometric titration procedure. This is because the condition $[\text{Cu}^{2+}]_{\text{T}} \gg [\text{L}]$ required for fitting eq 3 to the experimental values of A vs $[\text{M}^{n+}]$ cannot be used. The increase of absorbance at 260 nm was almost

Table 1. Association Constants (30 °C, $\mu = 1.0$) of Complexes of the Nucleotides, Their Leaving Alcohols, and 8-Hydroxy-2-methylquinoline^a and pK_{a} values of Phenolic Proton Ionization

	pK_{a}^b	$\text{Zn}^{2+ c}$	$\text{Mg}^{2+ d}$	La^{3+}
$\log K_{\text{as}} (\mathbf{1aH}_{-1}\text{M})$	9.73	7.04	3.03	ND ^e
$\log K_{\text{as}} (\mathbf{1bH}_{-1}\text{M})$	9.92	7.27	2.60	ND ^e
$\log K_{\text{as}} (\mathbf{7aH}_{-1}\text{M})$	9.61	7.81	2.52	7.35 ^f
$\log K_{\text{as}} (\mathbf{7bH}_{-1}\text{M})$	9.82	7.83	3.60	5.18 ^g
$\log K_{\text{as}} (\mathbf{8H}_{-1}\text{M})$	10.04	7.60	3.09	<4.00 ^h

^a $K_{\text{as}} (\text{LH}_{-1}) = [\text{LH}_{-1}\text{M}]/[\text{LH}_{-1}][\text{M}]$. ^b Acid dissociation constants (30 °C, $\mu = 1.0$) of the phenolic protons of the hydroxyquinoline moieties, determined by spectrophotometric pH titration (see Experimental Section). ^c Averaged values from the titration at pH 6.17 and 6.47. ^d Values from the titration at pH 8.8, except for **1bH}_{-1}\text{Mg} (pH 9.33). ^e Not determined. ^f Averaged value from the titration at pH 5.59, 6.05, and 6.47. ^g Value at pH 6.52. ^h From ref 15b.**

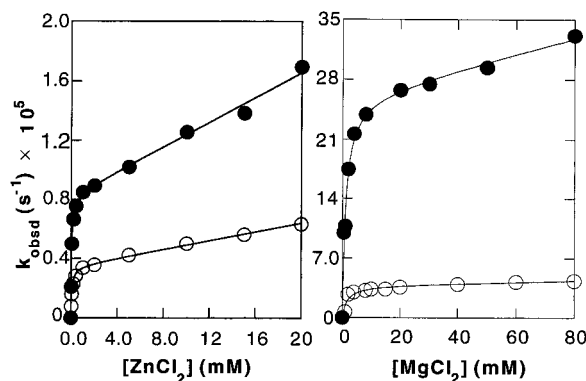


Figure 2. Dependence of the pseudo-order-rate constant (k_{obsd}) for hydrolysis of **1a** (●) and **1b** (○) on $[\text{Zn}^{2+}]$ (pH 6.50) and $[\text{Mg}^{2+}]$ (pH 9.83 with **1a** and pH 9.56 with **1b**) at 30 °C. The solid lines were created by using eq 6.

saturated at a concentration of Cu^{2+} four times that of $[\text{L}]$ with **1a**, **7a**, and **8** at pH 5.54 and for **1b** and **7b** at pH 6.2. Thus, we are unable to state with any certainty that complexes with a 1:1 stoichiometry are formed with Cu^{2+} .

Metal Ion-Promoted Hydrolysis. Hydrolyses of **1a** and **1b** in the presence of increasing concentrations of Zn^{2+} , Mg^{2+} , La^{3+} , and Cu^{2+} were investigated at 30 °C ($\mu = 1.0$ with KCl) and constant pH. Rates of the metal ion-promoted hydrolysis of **1a** and **1b** were essentially independent of the concentrations of the buffers employed (MES, HEPES, and CHES) when varied over a 10-fold change. The reactions involving Zn^{2+} , Mg^{2+} , and Cu^{2+} were followed by HPLC. All the reactions produced (8-hydroxyquinolyl)methanol (**7a**) or -ethanol (**7b**), depending on which nucleotide was used, and 2',3'-cyclic AMP together with minor products 2'-AMP and 3'-AMP. The identity of these products was established by comparison of their retention times with those of authentic samples. The minor species 2'- and 3'-AMP were produced in roughly equal amounts and presumably result from the subsequent hydrolysis of 2',3'-cyclic AMP. For La^{3+} -promoted hydrolysis of **1a** and **1b**, the reactions were so fast that stopped-flow spectrophotometry was required in order to follow the time course of the reactions (see Experimental Section). In what follows, the term "hydrolysis" or "hydrolytic cleavage" refers to rate-determining intramolecular transesterification by the 2'-OH group to provide directly the 2',3'-cyclic AMP intermediate.

Plots of the pseudo-first-order rate constants (k_{obsd}) vs metal ion concentration are shown in Figure 2 for hydrolysis of **1a** and **1b** in the presence of Zn^{2+} (pH 6.50) and Mg^{2+} (pH 9.83 for **1a**, pH 9.56 for **1b**) and in Figure 3 for La^{3+} (pH 7.43 for **1a**, pH 7.50 for **1b**). Examination of Figures 2 and 3 shows that hydrolysis of **1a** and **1b** exhibit a biphasic dependence on metal ion concentration. Both phases, at a given constant pH,

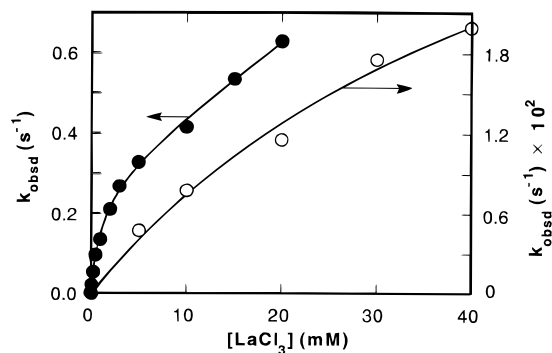
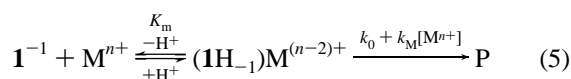


Figure 3. Influence of $[\text{La}^{3+}]$ on the pseudo-first-order rate constant (k_{obsd}) for hydrolysis of **1a** (●) and **1b** (○) at 30 °C ($\mu = 1.0$). The lines are nonlinear least-squares fits to the data points by use of eq 6. The constriction $k_{\text{M}} = 0$ was used for **1b**.

are linearly dependent upon metal ion concentration. The dependence of k_{obsd} on metal ion concentration can be described by preequilibrium formation of a reactive 1:1 metal–ligand complex that undergoes both spontaneous (k_0) and metal ion-catalyzed ($k_{\text{M}}[\text{M}]$) hydrolysis (eq 5).



The pseudo-first-order rate expression of eq 6 follows from eq 5. In eq 6, k_0 denotes the first-order rate constant for

$$k_{\text{obsd}} = (k_0 + k_{\text{M}}[\text{M}^{n+}])K_{\text{m}}[\text{M}^{n+}]/(a_{\text{H}} + K_{\text{m}}[\text{M}^{n+}]) \quad (6)$$

spontaneous hydrolysis of $(\mathbf{1H}_{-1})\text{M}^{(n-2)+}$, k_{M} the second-order rate constant for metal ion-catalyzed hydrolysis of the complex, $[\text{M}^{n+}]$ the total concentration of the metal ion, K_{m} association constant for formation of the 1:1 metal ligand complex, and a_{H} the proton activity of the reaction solution. This equation was used to fit the data points of the plots of k_{obsd} vs $[\text{M}^{n+}]$ in order to obtain the kinetic constants K_{m} , k_0 , and k_{M} (Figures 2 and 3). For the Mg^{2+} -promoted hydrolysis of **1b** (Figure 2, right side, open circle), the constriction of $k_{\text{M}} = 0$ was applied for the curve fitting, since the slope of the plots of k_{obsd} vs $[\text{Mg}^{2+}]$ is essentially zero at the higher metal ion concentrations. The satisfactory fit with this constriction indicates that the hydrolysis of the species $(\mathbf{1bH}_{-1})\text{Mg}$ is not measurably catalyzed by free Mg^{2+} . The same constriction was also applied to the fitting for the La^{3+} -promoted hydrolysis of **1b** (Figure 3, open circle), though little can be made of this since the magnitude of the rate constants restricts the concentration range of La^{3+} that can be used.

Plots of k_{obsd} vs metal ion concentration for Cu^{2+} -promoted hydrolysis (pH 6.05) of **1a** and **1b** are shown in Figure 4. At the concentrations of Cu^{2+} employed, **1a** and **1b** are entirely converted into copper complexes (see binding studies). No influence of the metal ion concentration on k_{obsd} was seen in the hydrolysis of the **1a** complex with Cu^{2+} (see inset in Figure 4), whereas the pseudo-first-order rate constant for hydrolysis of the **1b** complex exhibits a linear dependence on $[\text{Cu}^{2+}]$. Thus, the hydrolysis of a copper complex of **1a** is not catalyzed by additional Cu^{2+} while the hydrolysis of the copper complex of **1b** is catalyzed by addition of Cu^{2+} . The concentration-independent value of k_{obsd} for **1a** and intercept of the line in the plots of k_{obsd} vs $[\text{Cu}^{2+}]$ for **1b** represent the first-order rate constants (k_0) for spontaneous hydrolysis of copper complexes of **1a** and **1b**, respectively. The slope of the line gives the second-order rate constant (k_{M} ; eq 5).

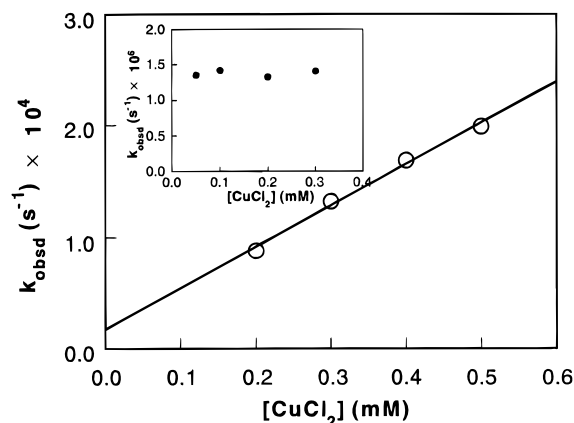


Figure 4. Dependence of the pseudo-first-order rate constant (k_{obsd}) for hydrolysis of **1a** on $[\text{Cu}^{2+}]$ (●, inset) and **1b** (○) at 30 °C ($\mu = 1.0$).

Table 2. Kinetic Constants (30 °C, $\mu = 1.0$) for the Hydrolysis of **1a** and **1b** with Various Metal Ions $\nu = k_0^{\text{HO}}[(\mathbf{1a} \text{ or } \mathbf{1b})\text{M}^{n+}][\text{HO}^-] + k_{\text{M}}^{\text{HO}}[(\mathbf{1a} \text{ or } \mathbf{1b})\text{M}^{n+}][\text{M}^{n+}][\text{HO}^-]$

nucleotide	metal	$\log K_{\text{as}}^a$	$k_0^{\text{HO}b}$ ($\text{s}^{-1} \text{M}^{-1}$)	$k_{\text{M}}^{\text{HO}b}$ ($\text{s}^{-1} \text{M}^{-2}$)
1a	Zn^{2+}	7.56	5.01×10^2	1.73×10^4
1a	Mg^{2+}	2.88	2.19	1.28×10^{-5}
1a	Cu^{2+}	ND ^c	8.49×10^1	~ 0
1a	La^{3+}	5.21	7.51×10^5	2.87×10^7
1b	Zn^{2+}	7.51	1.87×10^2	7.92×10^3
1b	Mg^{2+}	2.61	8.62×10^{-1}	~ 0
1b	Cu^{2+}	ND ^c	$\sim 10^1$ ^d	2.29×10^7
1b	La^{3+}	3.78	1.16×10^5	ND ^c

^a Kinetically determined by use of eq 6. ^b Determined by use of eqs 7 and 8. ^c Not determined. ^d Roughly estimated value. See text.

The dependence of k_{obsd} on $[\text{M}^{n+}]$ seen in Figures 2–4 is typical of the plots of k_{obsd} vs $[\text{M}^{n+}]$ for each metal ion catalysis of the hydrolysis of **1a** over the pH ranges studied. The values of k_0 and k_{M} are obtained from plots of k_{obsd} vs $[\text{M}^{n+}]$ at several different pH. Plots of the \log of k_{M} and k_0 vs pH are shown in Figure 5 (closed symbols) for hydrolysis of **1a** by each metal ion. These pH–rate profiles show a linear relationship with a slope of +1. The lines in Figure 5 show best fits to the data points with use of eqs 7 and 8 on the basis of the first-order dependence on $[\text{HO}^-]$ ($K_{\text{w}} = 10^{-13.8326}$).

$$k_0 = k_0^{\text{HO}}[\text{HO}^-] = \frac{k_0^{\text{HO}}K_{\text{w}}}{a_{\text{H}}} \quad (7)$$

$$k_{\text{M}} = k_{\text{M}}^{\text{HO}}[\text{HO}^-] = \frac{k_{\text{M}}^{\text{HO}}K_{\text{w}}}{a_{\text{H}}} \quad (8)$$

The values of k_0^{HO} and k_{M}^{HO} , used to create the best fit, are listed in Table 2. The kinetically determined values of K_{as} (Table 2)—obtained from the kinetic values of K_{m} by dividing by K_{a} —are roughly consistent with those determined thermodynamically. For the metal ion-promoted hydrolysis of **1b** a kinetic study was carried out, except with Cu^{2+} , at only a single pH. The points of the \log of k_0 and k_{M} for the metal ion-promoted hydrolysis of **1b** are included in Figure 5 (open symbols). Assuming the same pH dependence of k_0 and k_{M} for metal ion-promoted hydrolysis of **1b** as determined for **1a**, we calculated the values of k_0^{HO} and k_{M}^{HO} using eqs 7 and 8. The results are also included in Table 2.

Hydrolysis of the Nucleotides 1a and 1b in the Absence of Metal Ions. EDTA (1 mM) was incorporated into the reaction solution to sequester traces of metal ion impurities, and

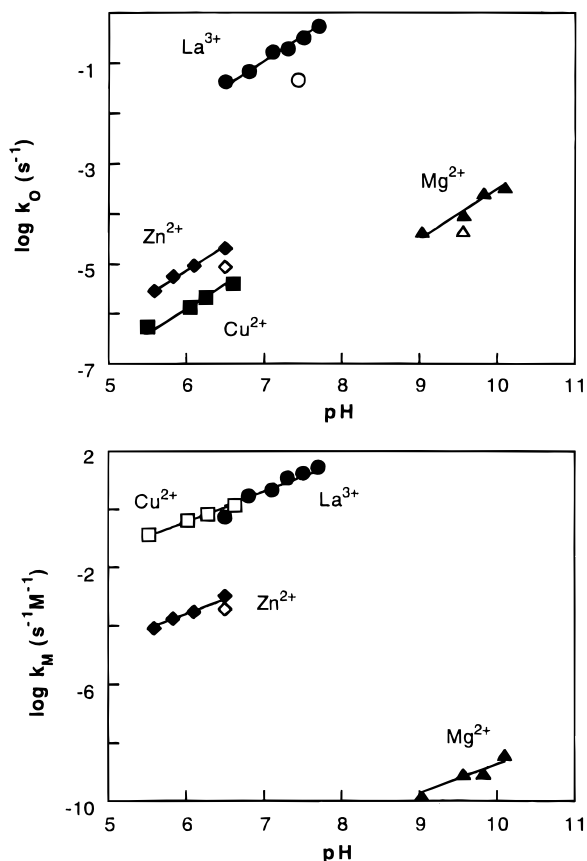
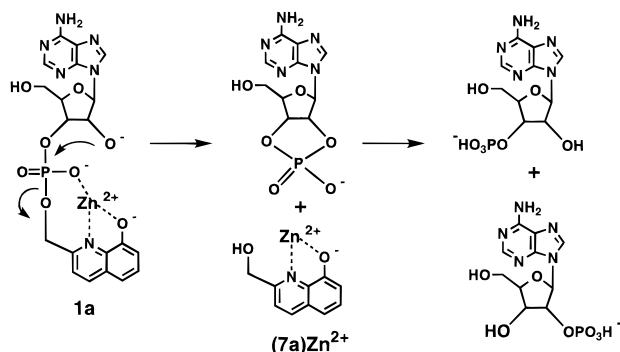


Figure 5. pH-rate profiles of the rate constant k_0 (top) and k_M (bottom) at 30 °C ($\mu = 1.0$) for hydrolysis of **1a** (closed symbols) and **1b** (open symbols) promoted by Zn^{2+} (◆), Mg^{2+} (▲), Cu^{2+} (■), and La^{3+} (●). The lines are drawn by use of eqs 7 and 8.

Scheme 2

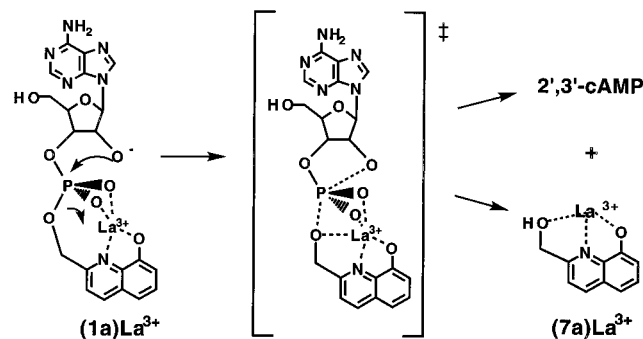


the hydrolysis of **1a** was studied at pH 7.0 and 30 °C ($\mu = 1.0$). The concentration of **1a** remained unchanged for 6 months. To estimate the reaction rate of hydrolysis of **1a** and **1b** without metal ions, we carried out the hydrolysis in 0.2 M KOH solution ($\mu = 1.0$ with KCl) at 30 °C. The second-order rate constants for reaction with HO^- were calculated as $7.5 \times 10^{-4} \text{ s}^{-1} \text{ M}^{-1}$ for **1a** and $3.1 \times 10^{-4} \text{ s}^{-1} \text{ M}^{-1}$ for **1b**.

Discussion

All of the metal ions (Mg^{2+} , Zn^{2+} , Cu^{2+} , and La^{3+}) tested promoted hydrolysis of the nucleotides **1a** and **1b** *via* intramolecular transesterification with formation of 2',3'-cyclic adenosine monophosphate and alcohols **7a** and **7b**, respectively (Scheme 2). The dependence of the pseudo-first-order rate constants (k_{obsd}) on metal ion concentration establishes involvement of two catalytic pathways (eq 5).¹⁸ The first is spontaneous hydrolysis (k_0) of the 1:1 metal ion complexes of **1a** and **1b**. In

Scheme 3



such complexes the metal ions are ligated by the 8-hydroxyquinoline moiety of **1a** and **1b**. With the exception of Cu^{2+} (see Results), the similarity of thermodynamically and kinetically determined association constants assures that reactive species are complexes with a 1:1 stoichiometry. In the second path the hydrolytic reaction is first order in the complexes (**1a**) Mn^+ or (**1b**) Mn^+ and first order in free metal ion. Thus, metal ion promotes hydrolysis ($k_M[\text{Mn}^+]$) of the 1:1 metal ion:ligand complexes.

The Structure of $\text{LM}^{\text{n}+}$ Complexes and the Mechanism of Their Hydrolysis by Lyate Species. In the ground state structure of the 1:1 complexes of metal ions with **1a** and **1b**, the negatively charged phosphodiester $-(\text{PO}_2^-)-$ moiety is much favored as a ligand, compared to the neutral oxygen, which becomes a leaving group. The metal ion in such 1:1 complexes can act as a Lewis acid catalyst, neutralizing the charge on the phosphate ester by ligation to one of the two (PO_2^-) oxygens and thereby activating the phosphorus atom toward nucleophilic attack (Scheme 2). In the single case of La^{3+} (*vide infra*), the metal ion may ligate to both oxygens of the (PO_2^-) entity as well as to the leaving oxygen (Scheme 3). Due to the formation of 2',3'-cyclic phosphate and the first-order dependence of the reaction rate on $[\text{HO}^-]$, the nucleophilic entity must be the anion of 2'-OH, which presumably attacks phosphate phosphorus inline with the leaving oxygen atom. Metal ion ligation to the oxygen of alkyl-OH lowers the pK_a of the latter thereby increasing the concentration of alkyl- O^- . In our model, however, metal ions Mg^{2+} , Zn^{2+} , and Cu^{2+} complexed to the 8-hydroxyquinoline moiety of **1a** and **1b** cannot easily ligate with the 2'-OH. This would require formation of 12- and 13-membered rings with proper orientation about six or seven single bonds in the metal complexes of **1a** and **1b**, respectively. Molecular modeling suggests that not only are these metal ions incapable of ligating with the nucleophile or the leaving group when complexed to the phosphodiester, but also water or hydroxide ligands in the metal ion's immediate coordination sphere cannot directly interact with the nucleophilic or leaving alcohols. For example, it is not possible for OH^- attached to Zn^{2+} in the (**1a**) Zn^{2+} or (**1b**) Zn^{2+} complexes to deprotonate the 2'-OH while retaining the correct geometry for inline attack on the phosphate, nor is it possible for H_2O attached to Zn^{2+} in the (**1a**) Zn^{2+} or (**1b**) Zn^{2+} complexes to protonate the leaving oxygen without disrupting phosphate coordination to the Zn^{2+} . This is so regardless of whether the metal ion is four-, five-, or six-coordinate.

(18) In a preliminary study,¹⁷ employing cacodylate buffer, it was found that (**1a**) Zn was not hydrolyzed by a mechanism involving two metals. This is due to the strong interaction of Zn^{2+} with this buffer species. Such an interaction would decrease the free metal ion concentration, inhibiting the second catalytic pathway. On the other hand, MES, HEPES, CHES, and CAPS buffers used in the present study are known to minimize the interaction with metal ions.

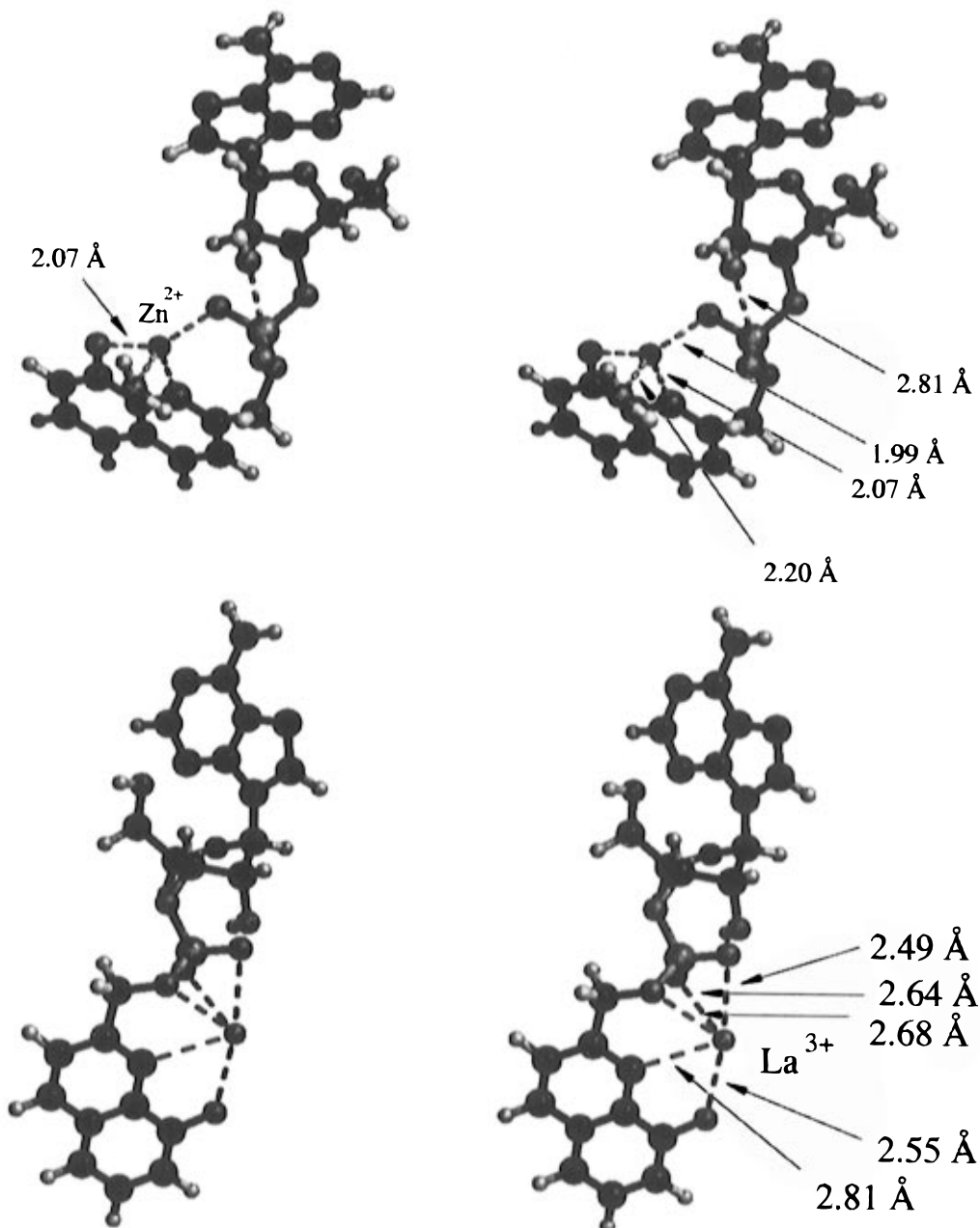


Figure 6. (Top) stereoview of the structure of **(1a)Zn** with the phosphate oxyanion ligated to the zinc at a bond length of 1.98 Å. The distance between Zn^{2+} and the leaving oxygen (3.36 Å) is too far for interaction, and any bonding would require distortion of the zinc tetrahedral structure. (Bottom) Stereoview of the structure of **((1a)La) $^{2+}$** . The distances between La^{3+} and both the leaving oxygen and phosphate oxyanion are suitable for interaction. In both the top and bottom structures, the 2'-OH is in position for an inline displacement of the leaving oxygen. The structures were built as follows: the X-ray structure of the complex of 8-hydroxyquinoline with Zn^{2+} (ref 29) was transferred from the Cambridge structural data base and linked at the 2-position of the quinoline ring to a energy-minimized structure of a Quanta-generated adenine-ribose- $\text{O}(\text{PO}_2^-)\text{OCH}_2\text{H}$ with the elimination of H_2 . For the La^{3+} complex, the $\text{La}-\text{O}$ and $\text{La}-\text{N}$ bond distances in 8-hydroxyquinoline chelation were adjusted to 2.55 and 2.67 Å, respectively. The torsion angles of the adenine-ribose- $\text{O}(\text{PO}_2^-)\text{OCH}_2\text{R}$ portion were manipulated to analyze the possible interactions.

Computer molecular modeling of the metal ion complexes has been carried out with the aid of the known structure of AMP esters and the X-ray structures of metal ion complexes of 8-hydroxyquinoline (Figure 6). Molecular modeling of the 1:1 complexes of **1a** and **1b** with divalent metal ions shows that interaction between the negative charge of the $-(\text{PO}_2^-)-$ oxygen and the metal ions ligated to the 8-hydroxyquinoline moiety is favored. This is so regardless of metal ions being tetrahedral Zn^{2+} , octahedral Mg^{2+} , or square planar Cu^{2+} . Interaction of metal ions with the leaving oxygen is also possible for 1:1 complexes of Mg^{2+} and Cu^{2+} but not with tetrahedral Zn^{2+} (Figure 6 (top)). Simultaneous interaction in the ground state, however, of Mg^{2+} or Cu^{2+} with both $>\text{PO}_2^-$ oxygen and leaving oxygen is impossible due to the rigid and well-oriented

geometry of these metal complexes. The same may be said about the possibility of pentameric Zn^{2+} ligating with an oxygen of $>\text{PO}_2^-$ as well as the leaving oxygen.

The situation is quite different in the case of the 1:1 complexes of **1a** and **1b** with La^{3+} . Molecular modeling of the 1:1 complex of La^{3+} with **1a** shows the ease in which this metal can simultaneously interact with both the $-(\text{PO}_2^-)-$ and leaving oxygen moieties (Figure 6 (bottom)). This is due to the greater $\text{La}^{3+}-\text{O}$ bond length (~ 2.60 Å)¹⁹ and, unlike transition metal ions, a lack of directionality of bonding by La^{3+} due to filled d-orbitals.²⁰

The spontaneous hydrolysis of the 1:1 complex of **1a**, and probably **1b**, with metal ions is first-order in $[\text{HO}^-]$ (eq 7). The bimolecular rate constants k_0^{HO} (eq 7) are sensitive to the identity

of the metal ion, varying by a factor of 10^6 ; the order of activity is $\text{La}^{3+} \gg \text{Zn}^{2+} > \text{Cu}^{2+} \gg \text{Mg}^{2+}$ in hydrolysis of the 1:1 metal complex of both **1a** and **1b** (Table 2). In general, Cu^{2+} is the most effective Lewis acid catalyst among divalent transition metal ions in the hydrolysis of carboxylic acid esters²¹ or pentavalent phosphorus compounds.²² This is due, at least in part, to the high association constants of Cu^{2+} complexes. Complex stability also explains the usual advantage of Zn^{2+} , as a Lewis acid catalyst compared to Mg^{2+} . For spontaneous hydrolysis of the complexes $(\mathbf{1})\text{M}^{n+}$, the Zn^{2+} complexes are more active than the Mg^{2+} complexes by a factor of 200 for both **1a** and **1b** and the Cu^{2+} complexes by a factor of 40 for **1a** and 10 for **1b**. The Zn^{2+} 1:1 complexes of **1a** and **1b** are more susceptible to lyate catalysis of hydrolysis than the corresponding Cu^{2+} species by ca. 1 kcal/mol. Rationalization of differences in ΔG^\ddagger amounting to a kcal or less are seldom assured. In the present case the differences in strain for the 8-hydroxyquinoline-complexed tetrahedral Zn^{2+} and square planar Cu^{2+} reaching the negative oxygen of $-(\text{PO}_2^-)-$ may be brought into consideration. For Cu^{2+} the square planar geometry requires a $\text{N}-\text{Cu}^{2+}-\text{O}$ angle of 90° . The angle and bond length for interaction of Zn^{2+} with negative $-(\text{PO}_2^-)-$ is exactly that required by the tetrahedral metal ion (Figure 6 (top)).

In our designs, we extended the methylene linker between the phosphate group and leaving oxygen of **1a** to an ethylene linker in **1b** to ascertain what would happen if the leaving oxygen could more closely approach the metal ion. In the hydrolysis of the metal complexes of **1b**, the interaction of the metal ions with the incipiently negatively charged leaving oxygen involves a six-membered cyclic transition state. The values of the rate constants (k_0^{HO}) for hydrolysis of $(\text{M}^{n+})\mathbf{1a}$ and $(\text{M}^{n+})\mathbf{1b}$ differ by less than 1 order of magnitude for any given M^{n+} . This shows that there is no significant difference in the transition states. Metal ion catalysis of hydrolysis of **1a** and **1b** is due, therefore, to interaction of metal ion with the negative charge of the phosphodiester. The small reduction of the reactivity on going from **1a** to **1b** is probably due to an increase in the flexibility of the (PO_2^-) -ligated cyclic 1:1 complex. On addition of a rotatable bond to $(\mathbf{1a})\text{M}^{n+}$ there is an extension of the seven-membered ring to the eight-membered ring of $(\mathbf{1b})\text{M}^{n+}$.

In comparison with the divalent metal ions studied, the ligation of La^{3+} has a more pronounced positive effect on the rates of hydrolysis of **1a** and **1b**. The values of k_0^{HO} for the hydrolysis of the complexes of **1a** and **1b** with La^{3+} are 10^3 times greater than k_0^{HO} of the Zn^{2+} complexes, whereas the kinetically determined association constants of La^{3+} complexes $(\mathbf{1a,b})\text{La}^{3+}$ are smaller than those of the $(\mathbf{1a,b})\text{Zn}^{2+}$ complexes by a factor of 10^2 . As supported by molecular modeling (Figure 6 (bottom)), this remarkable activity must originate from a combination of Lewis acid catalysis by coordination to the phosphate oxyanion and by interaction with the putative charge on the leaving oxygen in the transition state associated with departure of the leaving group. The interaction between La^{3+} and the leaving oxygen can be appreciated from the following observations. The association constants of La^{3+} with **7a** and

7b are greater than the dissociation constant of La^{3+} with **8**. This observation establishes that the lanthanum of the 8-hydroxyquinoline La^{3+} complexes in **1a** and **1b** can interact productively with the leaving oxygen during hydrolysis. Catalysis of hydrolysis of phosphate esters by metal ion-assisted departure of the leaving oxygen is well documented.²³

Rate enhancements for hydrolysis of the phosphodiester **1a** and **1b** brought about by metal ion complexation can be obtained from the ratios of the rate constants for hydroxide ion hydrolysis (k_0^{HO}) of metal complexed and non complexed esters. The rate enhancement for hydrolysis of **1a,b** by complexation with metal ions is as follows: $\sim 10^5$ with Zn^{2+} , $\sim 10^3$ with Mg^{2+} , $\sim 10^5$ with Cu^{2+} , and $\sim 10^9$ with La^{3+} . A rate acceleration of 10^5 for Zn^{2+} complexes is comparable to that proposed by Westheimer¹ in Lewis acid catalysis by cancellation of negative charge on oxygen atom of the phosphodiester. For the La^{3+} complexes the remarkable rate enhancement exceeding 10^5 results from the additional interaction of La^{3+} with the leaving oxygen, as described above.

The Mechanism of Hydrolysis of LM^{n+} Complexes by M^{n+} . The complexes $(\mathbf{1a})\text{M}^{n+}$ and $(\mathbf{1b})\text{M}^{n+}$ are themselves hydrolyzed by metal ion catalysis ($k_{\text{M}}[\text{M}^{n+}]$ in eq 5). The pH-rate profile for this catalytic pathway establishes the reaction to be first-order in $[\text{HO}^-]$ indicating a transition state composition of $[(\mathbf{1a,b})\text{M}^{n+}][\text{M}^{n+}][\text{HO}^-]$. We assume the kinetic equivalent $[(\mathbf{1a,b})\text{M}^{n+}][\text{M}^{n+}\text{OH}]$ to represent the reacting species and derive the rate constants (eq 8) as k_{M}^{HO} (Table 2). Values of the rate constants for hydrolysis of $(\mathbf{1a})\text{M}^{n+}$ and $(\mathbf{1b})\text{M}^{n+}$ are strongly dependent upon the nature of M^{n+} . Thus, k_{M}^{OH} for $\text{Zn}^{2+}(\text{HO})$ -catalyzed hydrolysis of $(\mathbf{1a})\text{Zn}^{2+}$ and $(\mathbf{1b})\text{Zn}^{2+}$ are quite comparable, whereas the values for k_{M}^{OH} for catalysis of hydrolysis of $(\mathbf{1a})\text{Mg}^{2+}$ and $(\mathbf{1b})\text{Mg}^{2+}$ by a second Mg^{2+} are both barely or not at all detectable. This difference in catalytic activity of Zn^{2+} and Mg^{2+} can be explained by the difference in the values of $\text{p}K_{\text{a}}$ for water ligated to each metal ion; $\text{p}K_{\text{a}}$ for $\text{Zn}(\text{H}_2\text{O})^{2+}$ is 9.5²⁴ and that for $\text{Mg}(\text{H}_2\text{O})^{2+}$ is 11.4.²⁵ These results suggest that metal hydroxide is a general base deprotonating the nucleophilic 2'-OH, while the substrate bound metal ion associates with the phosphate oxyanion. A combination of Lewis acid/general base catalysis is known in the intramolecular transesterification of phosphate esters²⁶

In contrast to the similarities in the reactivity of $(\mathbf{1a})\text{M}^{n+}$ and $(\mathbf{1b})\text{M}^{n+}$, when M^{n+} represents Zn^{2+} and Mg^{2+} , the hydrolysis of the complex $(\mathbf{1a})\text{Cu}^{2+}$ is not catalyzed by a second Cu^{2+} while the value of k_{M}^{HO} for the reaction of $(\mathbf{1b})\text{Cu}^{2+}$ with a second Cu^{2+} is ca. $10^7 \text{ M}^{-2} \text{ s}^{-1}$. Hence, some sort of geometrical feature of the substrate is important in determining the facility of second metal ion catalysis in the instance of Cu^{2+} . It has been known that $\text{Cu}(\text{HO})^+$ exists in polymeric species²⁷ at neutral pH due to a $\text{p}K_{\text{a}}$ value (7.22)²⁸ considerably lower than those for other metal ions tested here. Accordingly, the concentration of monomeric copper hydroxide $\text{Cu}(\text{HO})^+$ is decreased below that anticipated from the reported value of $\text{p}K_{\text{a}}$

(19) Guerriero, P.; Casellato, U.; Sitrán, S.; Vigato, P. A.; Graziani, R. *Inorg. Chem. Acta* **1987**, *133*, 337.

(20) Sinha, S. P. *Structure and Bonding*; Springer-Verlag: New York, **1989**; Vol. 25, p 69.

(21) (a) Steinberger, R.; Westheimer, F. H. *J. Am. Chem. Soc.* **1951**, *73*, 429. (b) Prue, J. E. *J. Chem. Soc.* **1952**, 2331.

(22) (a) Morrow, J. R.; Trogler, W. C. *Inorg. Chem.* **1988**, *27*, 3387. (b) Steffens, J. J.; Sampson, E. J.; Siewers, I. J.; Benkovic, S. J. *J. Am. Chem. Soc.* **1973**, *95*, 936. (c) Steffens, J. J.; Siewers, I. J.; Benkovic, S. J. *Biochemistry* **1975**, *14*, 2431. (d) Courteny, R. C.; Gustafson, R. L.; Westerback, S. J.; Hyytiäinen, H.; Chaberek, S. C., Jr.; Martell, A. E. *J. Am. Chem. Soc.* **1957**, *79*, 3030.

(23) (a) Murakami, Y.; Takagi, M. *J. Am. Chem. Soc.* **1969**, *91*, 5131.

(b) Murakami, Y.; Sunamoto, J. *Bull. Chem. Soc. Jpn.* **1971**, *44*, 1827. (c) Fife, T. H.; Pujari, M. P. *J. Am. Chem. Soc.* **1988**, *110*, 7790. (d) De Rosch, M. A.; Trogler, W. C. *Inorg. Chem.* **1990**, *29*, 2409.

(24) Rabenstein, D. L.; Blakney, G. *Inorg. Chem.* **1973**, *12*, 128.

(25) Basolo, F.; Pearson, R. G. *Mechanisms of Inorganic Reactions*; Wiley: New York, 1967.

(26) Bashkin, J. K.; Jenkins, L. A. *Comments Inorg. Chem.* **1994**, *16*, 77.

(27) Burgess, J. *Metal Ions in Solution*; Wiley and Sons: New York, 1978.

(28) Kakihana, H.; Amaya, T.; Maeda, M. *Bull. Chem. Soc. Jpn.* **1970**, *43*, 3155.

(29) (a) Merritt, L. L.; Cady, R. T.; Mundy, B. W. *Acta Crystallogr.* **1954**, *7*, 473. (b) Palenik, G. J. *Acta Crystallogr.* **1964**, *17*, 696.

(7.22) of H_2O ligated to Cu^{2+} at a given pH. On the assumption that the catalytic species is $\text{Cu}(\text{HO})^+$, therefore, the determined values of k_M^{HO} would be incorrectly small. On the other hand, the actual catalyst may well be the polymeric species of copper hydroxide. If so, the difference in catalytic activity of Cu^{2+} in the hydrolysis of **(1a)** Cu^+ and **(1b)** Cu^+ might be explained by the structure of a cupric oxide gel? Because of the facility of La^{3+} -catalyzed hydrolysis of **1a,b** we were not able to investigate the dependence of k_{obsd} over a sufficient range of $[\text{La}^{3+}]$ to allow comparison of k_M^{HO} (Table 2) for **(1a)** La^{2+} and **(1b)** La^{2+} . La^{3+} catalysis is only reported for **(1a)** La^{2+} .

Biological Implications. A two-metal ion mechanism has recently been proposed^{6a} for ribozyme-mediated hydrolysis of RNA. In the instance of hammerhead ribozyme, it has been

proposed that magnesium hydroxide acts as a base to deprotonate the 2'-OH group at a ribose ring for nucleophilic attack on the phosphorus atom. Another Mg^{2+} coordinates both to the negative charge on $-(\text{PO}_2^-)-$ and to the leaving oxygen such that this Mg^{2+} facilitates both 2'-O⁻ attack and departure of the leaving oxygen.⁶ This two-metal ion catalysis, which is a combination of Lewis acid/general base catalysis, is essentially identical to our proposed mechanism for the two La^{3+} -mediated hydrolysis of **(1)** M^{2+} .

Acknowledgment. We thank the office of Naval Research and the National Institutes of Health for financial support.

JA9607300